The Kinematics of Multi-Fingered Manipulation

David J. Montana
Bolt Beranek and Newman, Inc.
70 Fawcett Street
Cambridge, MA 02138

Abstract

Previously, general models of the kinematics of multi-fingered manipulation have only treated instantaneous motion (i.e., velocities). However, such models, which ignore the underlying configuration (or state) space, are inherently incapable of capturing certain properties of the fingers-plus-object system important to manipulation. In this paper, we derive a configuration-space description of the kinematics of the fingers-plus-object system. To do this, we first formulate contact kinematics as a "virtual" kinematic chain. Then, the system can be viewed as one large closed kinematic chain composed of smaller chains, one for each finger and one for each contact point. We examine the underlying configuration space and two ways of moving through this space. The first, kinematics-based velocity control, is a generalization of some previous velocity-based approaches. The second, hyperspace jumps, is a purely configuration-space concept. We conclude with a discussion of how these concepts can be used to understand the task of twirling a baton [6].

1 Introduction

A robot hand with multiple fingers grasping an object is a complex system whose kinematics are difficult to model. Each finger is an independent kinematic chain with multiple degrees of freedom. Plus, there are additional degrees of freedom asociated with the relative motion of the object and finger at each point of contact. (As we discuss in Section 2.3, each point of contact contributes five degrees of freedom.) The degrees of freedom add up very quickly even for simple hands. For example, the Stanford/JPL hand [18], which has three fingers with three joints each, has 9 finger degrees of freedom and 15 contact degrees of freedom for a total of 24 degrees of freedom. Complicating things further is the fact that the contact degrees of freedom are passive, i.e. they do not have an associated actuator to control them directly. Therefore, they require indirect control via appropriate kinematic and/or dynamic constraints. However, despite the inherent complexities, there has been significant progress in developing models of the kinematics of multi-fingered manipulation appropriate for control. We now summarize some previous work in this area and then present an overview of the contributions of this paper.

1.1 Previous Work

We can divide the general approaches to multi-fingered manipulation into two categories, those which focus solely on velocity and those which deal with configuration-space issues. The velocity-based approaches can be further divided into those which use purely kinematic control and those which rely on dynamic control. (By kinematic control, we mean that the state of the fingers-plus-object system is completely determined by the state of the finger joints and hence can be controlled by controlling the finger joints. By dynamic control, we mean the opposite, i.e., that the state of the full system depends on dynamic quantities as

well as the state of the finger joints.) Finally, the velocity-based approaches can also be divided into those which control the location of the object and those which control the position of the points of contact.

The majority of the work in multi-fingered manipulation has been of the kinematics-based, velocity-based, object-control variety. Salisbury [18] was the first to provide a method to convert a desired velocity for an object in the grasp of multiple fingers to the joint velocities of the fingers needed to achieve this object velocity. He defined the grasp matrix as a way to transform from object velocity to fingertip velocity. Kerr and Roth [11] added the following observations. First, they explicitly stated that the contact degrees of freedom are instantaneously equivalent to a spherical joint (and hence form what we call a "virtual joint") when the contacts are (in Salisbury's nomenclature) point contacts with friction. Second, they showed that the points of contact move across the object and fingertips during manipulation and incorporated this motion of the points of contact into their formulation. Hunt and Torfason [8] introduced the concept of the fingers-plus-object system as a closed kinematic chain with the contact degrees of freedom as spherical joints in this mechanism, and Hunt, Samuel and McAree [9] have analyzed special configurations of this closed kinematic chain. (We take this idea of a closed kinematic chain from the velocity domain to the configuration-space domain.) Li, Murray and Sastry [12], [17] discuss how the constraints on the system need not be those for hard fingertips with friction but can be arbitrary kinematic constraints. (We generalize even further to allow dynamic constraints.)

Some other velocity-based approaches are the following. The work by Montana [15], [14] is an example of the kinematics-based, contact-control approach. It discusses how to control the positions of the points of contacts for a two-fingered grasp with soft fingertips with friction. (We generalize this to arbitrary constraints and an arbitrary number of fingers.) "Controlled slip" is an example of the dynamics-based approach. In controlled slip, the velocities of the contact degrees of freedom are kinematically underconstrained and are hence determined by the dynamics of the system and the external forces and torques. Brock [1] discusses the kinematics of controlled slip and in particular how to determine the subspace of possible instantaneous motions for a given grasp configuration. Cole, Hsu and Sastry [5] go further and model the dynamics of the system and thus provide a way to predict which of the possible velocities the system will have. They use this to control the positions of the contact points.

Some work requiring a full configuration-space description is the following. Fearing [6] desribes the task of twirling a baton. This requires disengagement of the fingers from contacting the object and re-engagement in a different configuration (which we call a "hyperspace jump"), a maneuver which cannot be described without a configuration-space formulation. Hong et al. [7] discuss the task of "striding," which uses four fingers to manipulate an object by grasping the object with one pair of fingers while the other pair moves to a new grasp location and then reversing the roles of the two pairs. This task also uses hyperspace jumps and hence requires a configuration-space description. Trinkle and Paul [19] describe a method for adjusting the grasp configuration while lifting an object. The non-local nature of the operation makes a configuration-space description necessary. Li and Canny [13] show that although the (nonholonomic) constraints on the contact degrees of freedom from soft fingertip with friction (or point contact with friction) constrain the velocities of the contact degrees of freedom to a proper subspace of their possible values, it is still in general possible to reach all the points of the underlying configuration space. They then show how to plan paths between any two points in the configuration space obeying the constraints. Some of Brock's work [1] on controlled slip deals with finite motions and hence with configuration-space concepts.

A good summary of much of the work on multi-fingered manipulation is [17].

1.2 Summary of Our Work

We derive a general description of the kinematics of multi-fingered manipulation which encompasses the kinematic analyses of many of the approaches described above as special cases. (One way in which our kinematic analysis is not fully general is that it assumes one contact point per finger and hence does not include analyses such as that in [19].) We start with a discussion of background information in Section 2. Section 2.1 briefly introduces basic concepts of rigid-body motion to establish terminology and notation. Section 2.2 discusses kinematic chains and their representations as labeled graphs called Euclidean graphs. Sections 2.1 and 2.2 largely follow the treatment of these subjects by Brockett [2]. Section 2.3 discusses contact kinematics, which is the relationship between the relative motion of two objects and the motion of their point of contact on their surfaces. This problem was originally solved by Montana [14], [15] and Cai and Roth [3], and our treatment here largely follows that of [15] with the important difference that here we formulate contact kinematics as a virtual kinematic chain.

Section 3 presents our description of the kinematics of multi-fingered manipulation. In Section 3.1, we show how these kinematics can be represented as a large, closed virtual kinematic chain whose components are the kinematic chains of the fingers and the virtual kinematic chains of the contact points. Section 3.2 discusses how the configuration space of the fingers-plus-object system is defined by the constraint that it forms a closed kinematic chain plus a group of additional constraints which we call the *generalized joint limits*. Sections 3.3 and 3.4 examine two ways to move throught configuration space using kinematics-based control. The first, kinematics-based velocity control, describes the situation when all the fingertips maintain contact with the object and the (unactuated) contact degrees of freedom and the object location evolve continuously as a function of the joint velocities. The second, *hyperspace jumps*, describes the case when some of the fingertips break contact with the object and then regain contact in another configuration. Note that we do not discuss dynamics-based control in this paper even though many instances of it fit within our general kinematic model. Section 3.5 examines the task of twirling a baton and how velocity control and hyperspace jumps can be used to plan a trajectory through configuration space which solves this task.

2 Background

2.1 Rigid-Body Motion

To represent the location (i.e., position and orientation) of a rigid body, we select a coordinate frame fixed with respect to the object, which we call the object's *body frame*. The relative location of two rigid bodies is given by the unique rigid (i.e., length-preserving) transformation which maps the "reference" object's body frame to the "moving" object's body frame. Such a transformation can be written as a 4x4 matrix of the form $T = \begin{bmatrix} R & \vec{d} \\ 0 & 1 \end{bmatrix}$, where $R \in \mathbf{SO}(3)$ (where $\mathbf{SO}(3)$ denotes the special orthogonal group in 3 dimensions, i.e. the set of 3x3 rotational matrices) and $\vec{d}$ is a 3-vector. When we represent transformations in this form, composing two transformations is equivalent to multiplying their matrix representations. Hence, if we have three coordinate frames C_1, C_2 and C_3, then $T_{12}T_{23} = T_{13}$, where T_{ij} is the matrix representation of the transformation from C_i to C_j. The set of all such transformations is the special Euclidean group in 3 dimensions $\mathbf{SE}(3)$.

As two rigid bodies move, their relative location will vary continuously as a function of time. This motion defines a curve $T : I \to \mathbf{SE}(3)$, where $I \subset \Re$ is an interval and $T(t)$ is the relative location at time t. The velocity of the motion relative to the moving body frame is $V = T^{-1}\dot{T}$. We can always write V in

the form $V = \begin{bmatrix} \Omega & \vec{v}_t \\ 0 & 0 \end{bmatrix}$, where Ω, the rotational velocity, is a 3x3 skew-symmetric matrix (i.e. $\Omega \in \mathbf{so}(3)$) and $\vec{v}_t$, the translational velocity, is a 3-vector. The set of all matrices of this form is the algebra $\mathbf{se}(3)$.

The velocity transforms from one coordinate frame to another via the map

$$\mathbf{ad}(\tilde{T}) : \mathbf{se}(3) \to \mathbf{se}(3), \qquad V \mapsto \tilde{T}^{-1} V \tilde{T} \tag{1}$$

where $\tilde{T} \in \mathbf{SE}(3)$ is the transformation from the original coordinate frame to the new coordinate frame. For example, the velocity relative to the reference body frame is

$$V' = \mathbf{ad}(T^{-1})V = T(T^{-1}\dot{T})T^{-1} = \dot{T}T^{-1} \tag{2}$$

We often prefer to write velocities as vectors rather than as matrices. If the rotational velocity matrix is $\Omega = \begin{bmatrix} 0 & -\omega_z & \omega_y \\ \omega_z & 0 & -\omega_x \\ -\omega_y & \omega_x & 0 \end{bmatrix}$, then we define the rotational velocity vector as $\vec{\omega} = \begin{bmatrix} \omega_x \\ \omega_y \\ \omega_z \end{bmatrix}$. Note that the map $* : \Re^3 \to \mathbf{SO}(3)$ such that $*\vec{\omega} = \Omega$ is called the Hodge * operator. To transform the 4x4 velocity matrix V to the six-vector $\vec{v} = \begin{bmatrix} \vec{v}_t \\ \vec{\omega} \end{bmatrix}$, we define the map

$$\gamma_1 : \mathbf{se}(3) \to \Re^6, \qquad V \mapsto \vec{v} \tag{3}$$

Changing coordinates induces a linear transformation of the velocity. Hence, for the 6-vector representation of velocity, any coordinate transformation can be represented as a 6x6 matrix. The function γ_2, defined as

$$\gamma_2 : \mathbf{SE}(3) \to \mathbf{GL}(6), \qquad \begin{bmatrix} R & \vec{d} \\ 0 & 1 \end{bmatrix} \mapsto \begin{bmatrix} R^T & -R^T(*\vec{d}) \\ 0 & R^T \end{bmatrix} \tag{4}$$

maps the 4x4 representation of a transformation matrix to a 6x6 representation such that for all $T \in \mathbf{SE}(3)$ and all $V \in \mathbf{se}(3)$,

$$\gamma_2(T)\gamma_1(V) = \gamma_1(\mathbf{ad}(T)(V)) \tag{5}$$

For further detail on this approach to rigid-body motion, see [2].

2.2 Euclidean graphs and kinematic chains

A Euclidean graph is a graph which has a coordinate frame associated with each node. We will use Euclidean graphs to represent constrained motion of multiple rigid bodies. Each node represents a rigid body, and an arc between two nodes represents a direct constraint on the relative motion of the two corresponding bodies. Each constraint limits the possible relative motion of the two bodies to a family of motions parametrized by a small number of variables. Hence, associated with each arc is a corresponding family of motions and a chosen parametrization for this family. In our figures, the arcs of Euclidean graphs show the associated parameters of the motion.

Euclidean graphs capture the structure of any mechanism consisting of joints and rigid links, a type of mechanism called a *kinematic chain*. The links of the mechanism are the nodes of the graph, and the joints are the arcs. Figure 1 shows a Euclidean graph depicting an example of a common robotic mechanism, an "open" kinematic chain. It is called "open" because its graph has no closed paths. From a kinematic viewpoint, what is of primary interest is the relationship between $\theta_1, ..., \theta_n$, the joint parameters, and T_{0n}, the transformation from C_0 to C_n, i.e. the relative location of the ends of the chain,

$$T_{0n} = T_1(\theta_1)T_2(\theta_2)...T_n(\theta_n) \tag{6}$$

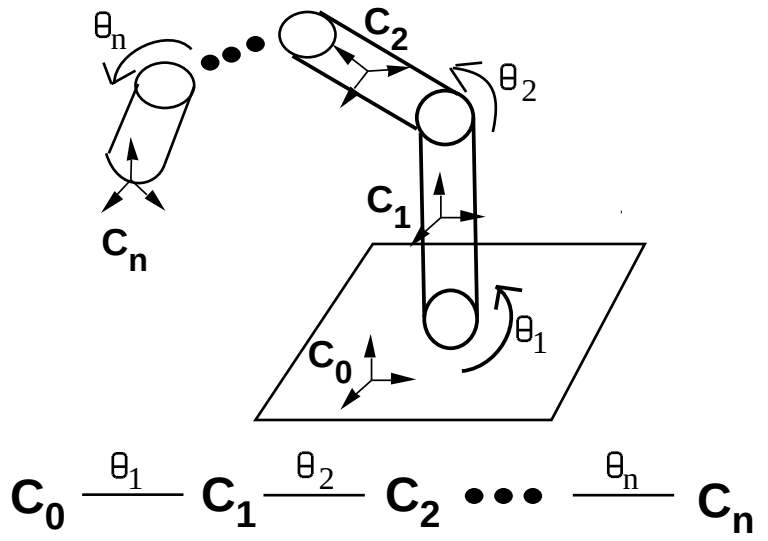

Figure 1: An open kinematic chain with its Euclidean graph.

where T_i maps the parameters θ_i into its corresponding transformation. The velocity is

$$V_{0n} = T_{0n}^{-1}\dot{T}_{0n} = \mathbf{ad}(T_2...T_n)(T_1^{-1}\dot{T}_1) + \mathbf{ad}(T_3...T_n)(T_2^{-1}\dot{T}_2) + ... + T_n^{-1}\dot{T}_n \tag{7}$$

$$\vec{v}_{0n} = \gamma_1(V_{0n}) = J \begin{bmatrix} \dot{\theta}_1 \\ \cdots \\ \dot{\theta}_n \end{bmatrix} \tag{8}$$

where J is a 6xn matrix called the *Jacobian*, given by

$$J = \begin{bmatrix} \gamma_2(T_2...T_n)\gamma_1(T_1^{-1}\frac{dT_1}{d\theta_1}), & \gamma_2(T_3...T_n)\gamma_1(T_2^{-1}\frac{dT_2}{d\theta_2}), & \cdots, & \gamma_1(T_n^{-1}\frac{dT_n}{d\theta_n}) \end{bmatrix} \tag{9}$$

The inverse of this kinematic chain, i.e. the transformation from C_n to C_0, is related to the original chain as

$$T_{n0} = T_{0n}^{-1}, \quad V_{n0} = -\mathbf{ad}(T_{0n}^{-1})V_{0n}, \quad J_{n0} = -\gamma_2(T_{0n}^{-1})J_{0n} \tag{10}$$

(Note that this is different from "inverse kinematics", which refers to solving Equation 6 for the joint parameters.)

Figure 2 shows a "closed" kinematic chain, i.e. a kinematic chain whose graph has at least one closed path. Each closed path adds a global constraint (as opposed to the local constraints represented by the arcs) that composition of the transformations around the closed path yields the identity transformation. For the example in Figure 2, this constraint is

$$I = T_0(\theta_0)T_1(\theta_1)...T_n(\theta_n) \tag{11}$$

Some mechanical systems which are not mechanisms consisting of links and joints can still be represented as Euclidean graphs. We call such a system a *virtual* kinematic chain. We now discuss an example of a virtual kinematic chain.

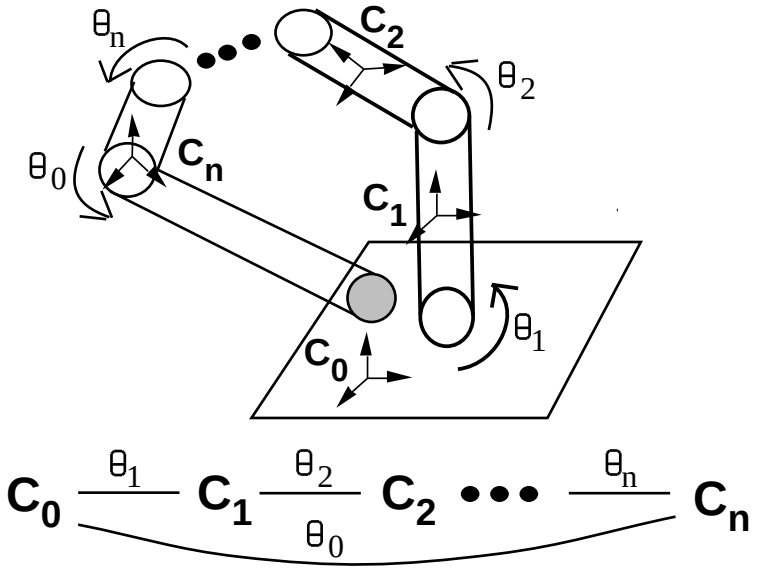

Figure 2: A closed kinematic chain with its Euclidean graph.

2.3 Contact Kinematics

We now consider two arbitrarily-shaped, rigid objects which move while maintaining contact between their surfaces. Assume that they contact at a single point. Then, their relative motion has five degrees of freedom. (The one constraint imposed by contact is that their relative motion have no translational component along their common surface normal.) We can view these five degrees of freedom as the sum of the following pieces: two degrees of freedom for the position of the point of contact on one object's surface, two degrees of freedom for its position on the other object's surface, and one degree of freedom of rotation around the common surface normal. We now show how to express the relative motion of the two objects as a composition of these three pieces and hence as a virtual kinematic chain.

Notation 1 For a function $f(u, v)$, f_u and f_v denote the partial derivatives of f with respect to u and v respectively.

Definition 1 A *coordinate patch* S_o for a surface $S \subset \Re^3$ is an open, connected subset of S with the following property: there exists an open subset $U \subset \Re^2$ and a diffeomorphism $f : U \to S_o \subset \Re^3$ such that the partial derivatives $f_u(\vec{u})$ and $f_v(\vec{u})$ are linearly independent for all $\vec{u} = (u, v) \in U$. The pair (f, U) is called a *coordinate system* for S_o. The *coordinates* of a point $s \in S_o$ are $(u, v) = f^{-1}(s)$ (see Figure 3).

Definition 2 A coordinate system (f, U) is *orthogonal* if $f_u(\vec{u}) \cdot f_v(\vec{u}) = 0$ for all $\vec{u} \in U$. We call (f, U) *right-handed* if $f_u(\vec{u}) \times f_v(\vec{u})$ is outwardly normal to the surface for all $\vec{u}$.

Definition 3 The *Gauss frame* (see Figure 4) for a right-handed orthogonal coordinate system (f, U) at a point $\vec{u} \in U$ is the coordinate frame with origin at $s = f(\vec{u})$ and coordinate axes

$$\vec{x}(\vec{u}) = f_u(\vec{u})/\|f_u(\vec{u})\|, \quad \vec{y}(\vec{u}) = f_v(\vec{u})/\|f_v(\vec{u})\|, \quad \vec{z}(\vec{u}) = \vec{x}(\vec{u}) \times \vec{y}(\vec{u}) \tag{12}$$

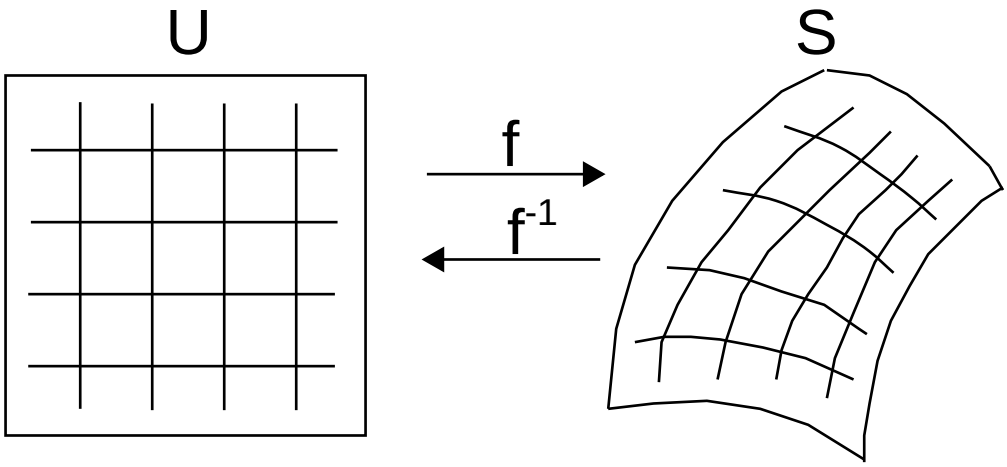

Figure 3: A coordinate system for a surface.

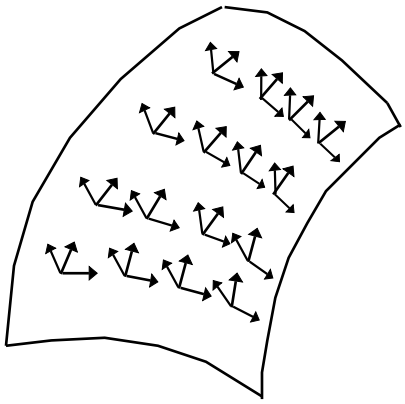

Figure 4: The Gauss frames for some points on the surface.

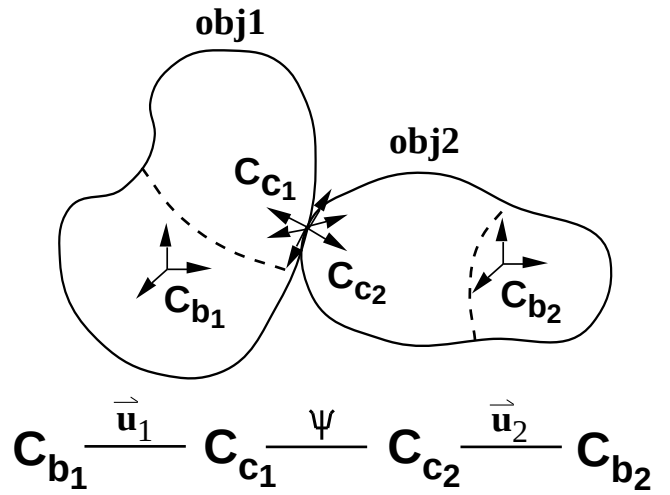

Figure 5: The coordinate frames for contact kinematics and their Euclidean graph.

Example 1 Consider the set

$$U = \{(u, v) | -\pi/2 < u < \pi/2, -\pi < v < \pi\} \tag{13}$$

and the map

$$f : U \to \Re^3 \qquad (u, v) \mapsto (\rho \cos u \cos v, -\rho \cos u \sin v, \rho \sin u) \tag{14}$$

for some $\rho > 0$. Let $S_o = f(U)$. The reader can verify that (f, U) is a right-handed orthogonal coordinate system for S_o. Let S be the sphere of radius ρ. Then, S_o is a coordinate patch for S. The coordinates u and v are known as the latitude and longitude respectively. The induced Gauss frame is

$$\vec{x}(\vec{u}) = \begin{bmatrix} -\sin u \cos v \\ \sin u \sin v \\ \cos u \end{bmatrix} \quad \vec{y}(\vec{u}) = \begin{bmatrix} -\sin v \\ -\cos v \\ 0 \end{bmatrix} \quad \vec{z}(\vec{u}) = \begin{bmatrix} \cos u \cos v \\ -\cos u \sin v \\ \sin u \end{bmatrix} \tag{15}$$

On the spherical surface of the earth, the x, y and z directions are called north, west and up respectively.

A Gauss frame associates a coordinate frame with a point on a surface. Therefore, it allows motion along a surface to be viewed as "virtual" rigid-body motion, which is the key to the following formulation of contact kinematics as a virtual kinematic chain.

Call the objects $obj1$ and $obj2$. Choose body frames C_{b_1} and C_{b_2} fixed relative to $obj1$ and $obj2$ respectively. Let $S_1 \subset \Re^3$ and $S_2 \subset \Re^3$ be the embeddings of the surfaces of $obj1$ and $obj2$ relative to C_{b_1} and C_{b_2} respectively. Choose right-handed, orthogonal coordinate systems (f_1, U_1) and (f_2, U_2) for coordinate patches $S_{10} \subset S_1$ and $S_{20} \subset S_2$ such that the points of contact stay within S_{10} and S_{20}. The coordinates of the point of contact on $obj1$ and $obj2$ are $\vec{u}_1(t)$ and $\vec{u}_2(t)$. Define the contact frames C_{c_1} and C_{c_2} to be the Gauss frames at $\vec{u}_1(t)$ and $\vec{u}_2(t)$ respectively (see Figure 5). Note that the z axis of C_{c_1} must always be the negative z axis of C_{c_2} because at the point of contact the outward normal to $obj1$ is the inward normal to $obj2$. Finally, define the contact angle $\psi(t)$ as the angle between the x axes of C_{c_1} and C_{c_2}. We choose the sign of ψ so that a rotation of C_{c_1} through angle $-\psi$ around its z axis alligns the x axes.

The Euclidean graph for contact kinematics is shown in Figure 5. This is a virtual five-degree-of-freedom kinematic chain. The first "joint" has two degrees of freedom and is parametrized by $\vec{u}_2$; the

second "joint" has one degree of freedom and is parametrized by ψ; the third "joint" has two degrees of freedom and is parametrized by $\vec{u}_1$. The transformation $T_2 \in \mathbf{SE}(3)$ which characterizes the first "joint" is

$$T_2 = \begin{bmatrix} \vec{x}_2(\vec{u}_2(t)) & \vec{y}_2(\vec{u}_2(t)) & \vec{z}_2(\vec{u}_2(t)) & f_2(\vec{u}_2(t)) \\ 0 & 0 & 0 & 1 \end{bmatrix} \tag{16}$$

where $\vec{x}_2(\vec{u}_2)$, $\vec{y}_2(\vec{u}_2)$ and $\vec{z}_2(\vec{u}_2)$ are the coordinate vectors of C_{c_2} relative to C_{b_2} and are as given in Equation 12. The transformation T_ψ which characterizes the second "joint" is

$$T_\psi = \begin{bmatrix} \cos\psi(t) & -\sin\psi(t) & 0 & 0 \\ -\sin\psi(t) & -\cos\psi(t) & 0 & 0 \\ 0 & 0 & -1 & 0 \\ 0 & 0 & 0 & 1 \end{bmatrix} \tag{17}$$

The inverse T_1 of the transformation which characterizes the third "joint" is

$$T_1 = \begin{bmatrix} \vec{x}_1(\vec{u}_1(t)) & \vec{y}_1(\vec{u}_1(t)) & \vec{z}_1(\vec{u}_1(t)) & f_1(\vec{u}_1(t)) \\ 0 & 0 & 0 & 1 \end{bmatrix} \tag{18}$$

where $\vec{x}_1(\vec{u}_1)$, $\vec{y}_1(\vec{u}_1)$ and $\vec{z}_1(\vec{u}_1)$ are the coordinate vectors of C_{c_1} relative to C_{b_1} and are as given in Equation 12. Combining these transformations yields the following

Theorem 1 *(Full Forward Kinematics) The transformation T from C_{b_2} to C_{b_1} can be written as*

$$T = T_2 T_\psi T_1^{-1} \tag{19}$$

To derive the instantaneous kinematics, we need the following definitions of geometric quantities

Definition 4 For a given orthogonal coordinate system (f, U), define the *curvature* K, the *torsion* Q, and the *scale matrix* M as

$$K = [\vec{x}(\vec{u}), \vec{y}(\vec{u})]^T [\vec{z}_u(\vec{u})/\|f_u(\vec{u})\|, \vec{z}_v(\vec{u})/\|f_v(\vec{u})\|] \tag{20}$$

$$Q = \vec{y}(\vec{u})^T [\vec{x}_u(\vec{u})/\|f_u(\vec{u})\|, \vec{x}_v(\vec{u})/\|f_v(\vec{u})\|] \tag{21}$$

$$M = \mathrm{diag}(\|f_u(\vec{u})\|, \|f_v(\vec{u})\|) \tag{22}$$

Intuitively, the curvature maps differential motions along the surface into the corresponding changes in the surface normal. The torsion measures the "twist" in the Gauss frame for a differential motion along the surface. The scale matrix transforms differential changes in coordinates into differential distances along the surface.

Example 2 Consider the coordinate system (f, U) from Example 1. The curvature, torsion form and scale form are

$$K = \begin{bmatrix} \frac{1}{\rho} & 0 \\ 0 & \frac{1}{\rho} \end{bmatrix} \qquad Q = \begin{bmatrix} 0 & \frac{-\tan u}{\rho} \end{bmatrix} \qquad M = \begin{bmatrix} \rho & 0 \\ 0 & \rho\cos u \end{bmatrix} \tag{23}$$

To formulate the instantaneous kinematics, we also need these definitions. The velocity V of the kinematic chain T is as defined in Section 2.1

$$V = T^{-1}\dot{T}, \qquad \vec{v} = \gamma_1(V) \tag{24}$$

We also define the *contact velocity* $\tilde{V}$ as

$$\tilde{V} = \mathbf{ad}(T_1)V, \qquad \tilde{\vec{v}} = [v_x, v_y, v_z, \omega_x, \omega_y, \omega_z]^T = \gamma_1(\tilde{V}) \tag{25}$$

The contact velocity is the velocity of the chain expressed relative to the frame C_{c_1}. This is a natural frame relative to which to express the velocity: pure sliding corresponds to $v_z = \omega_x = \omega_y = \omega_z = 0$, pure rolling contact corresponds to $v_x = v_y = v_z = \omega_z = 0$, and pure twist corresponds to $v_x = v_y = v_z = \omega_x = \omega_y = 0$.

Let $\vec{\phi} = \begin{bmatrix} \vec{u}_1 \\ \vec{u}_2 \\ \psi \end{bmatrix}$ be the vector of contact parameters. Let K_1, Q_1 and M_1 be the curvature, torsion form, and scale form for the coordinate system (f_1, U_1) at $\vec{u}_1(t)$. Define K_2, Q_2 and M_2 analogously. Finally, let

$$R_\psi = \begin{bmatrix} \cos\psi & -\sin\psi \\ -\sin\psi & -\cos\psi \end{bmatrix} \qquad R_0 = \begin{bmatrix} 0 & 1 \\ -1 & 0 \end{bmatrix} \tag{26}$$

Theorem 2 *(Instantaneous Forward Kinematics)*

$$\tilde{\vec{v}} = \tilde{J}\dot{\vec{\phi}} \tag{27}$$

where the matrix $\tilde{J}$ is given by

$$\tilde{J} = \begin{bmatrix} -M_1 & R_\psi M_2 & 0 \\ 0 & 0 & 0 \\ R_0 K_1 M_1 & R_0 R_\psi K_2 M_2 & 0 \\ -Q_1 M_1 & -Q_2 M_2 & 1 \end{bmatrix} \tag{28}$$

Theorem 2 is proven in [15]. Furthermore, in [15], the matrix $\tilde{J}$ is inverted, and hence the inverse kinematics are derived (and referred to as the contact equations).

Corrolary to Theorem 2 *$\vec{v} = J\dot{\vec{\phi}}$, where J is the Jacobian and is given by*

$$J = \gamma_2(T_1^{-1})\tilde{J} \tag{29}$$

3 Multi-fingered Manipulation

We now investigate the problem of manipulating a rigid object with multiple fingers, each of which is a multi-jointed kinematic chain. We will assume that the contact between the object and each finger occurs at a single point in the final link (which we henceforth call the fingertip) of the finger. Manipulation consists of changing the state of the system in some "controlled" manner.

Section 3.1 formulates a general description of the kinematics as a large closed, virtual kinematic chain. Section 3.2 examines the configuration space and the "generalized joint limits" which constrain the space. Sections 3.3 and 3.4 discuss two ways to move through configuration space. Section 3.3 describes a general approach to velocity control, in particular how to indirectly control the contact degrees of freedom, which are not actuated. Section 3.4 discusses "hyperspace jumps", which are another method for moving through configuration space. Section 3.5 describes how to use kinematics-based velocity control and hyperspace jumps to perform the task of twirling a baton.

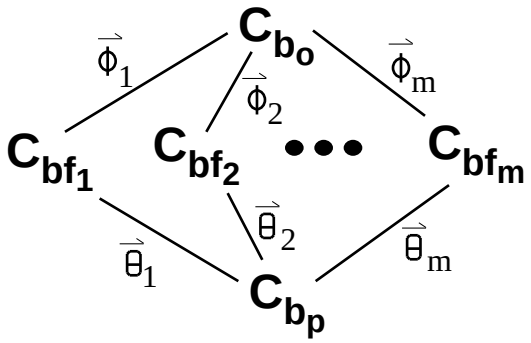

Figure 6: The Euclidean graph for multi-fingered manipulation (note that each arc of this graph can be expanded into a subgraph of the form shown in either Figure 1 or Figure 5).

3.1 Kinematics of the Fingers-Plus-Object System

Define the following coordinate frames. C_{bp} is the body frame of the palm of the hand. C_{bo} is the body frame of the object. $C_{bf_1}, ..., C_{bf_m}$ are the body frames for each of the m fingertips. $C_{cf_1}, ..., C_{cf_m}$ are the contact frames for the fingertips. $C_{co_1}, ..., C_{co_m}$ are the contact frames for the object at each of the m points of contact.

We can represent the full kinematics of the system (fingers plus object) as the closed Euclidean graph in Figure 6. Each arc of this graph actually represents an open kinematic subchain. The arc from C_{bf_i} to C_{bp} represents the kinematic chain of finger i. Because each finger is a multi-jointed mechanism, it has the form shown in Figure 1. We call the vector of its internal joint parameters $\vec{\theta}_i$. The arc from C_{f_i} to C_{bo} represents the virtual kinematic chain for the contact kinematics of the object and finger i. This chain's graph has the form shown in Figure 5. We call the vector of its internal joint parameters $\vec{\phi}_i = \begin{bmatrix} \vec{u}_{f_i} \\ \vec{u}_{o_i} \\ \psi_i \end{bmatrix}$ As an example, Figure 7 shows all the coordinate frames and the full Euclidean graph for a planar manipulator consisting of two finger each with two joints and flat fingertips. The y directions for all coordinate frames in this example point into the page.

We can think of each of the m paths from C_{bp} to C_{bo} as being an "extended" finger whose "joints" are the physical joints of the finger plus the contact degrees of freedom. Each extended finger has $n_i + 5$ degrees of freedom, where n_i is the number of physical joints of finger i. The kinematics of an exteded finger are as follows. The state vector is $\begin{bmatrix} \vec{\theta}_i \\ \vec{\phi}_i \end{bmatrix}$. The transformation for a given state is

$$T_{e_i}(\begin{bmatrix} \vec{\theta}_i \\ \vec{\phi}_i \end{bmatrix}) = T_{f_i}(\vec{\theta}_i) T_{c_i}(\vec{\phi}_i) \tag{30}$$

where T_{f_i} and T_{c_i} are the transformations for the finger and contact subchains respectively. The velocity is given by

$$\vec{v}_{e_i} = \gamma_2(T_{c_i}) J_{f_i} \dot{\vec{\theta}}_i + J_{c_i} \dot{\vec{\phi}}_i \tag{31}$$

where J_{f_i} and J_{c_i} are the Jacobians of the subchains. Hence, the Jacobian for the extended finger is

$$J_{e_i} = [\gamma_2(T_{c_i}) J_{f_i}, J_{c_i}] \tag{32}$$

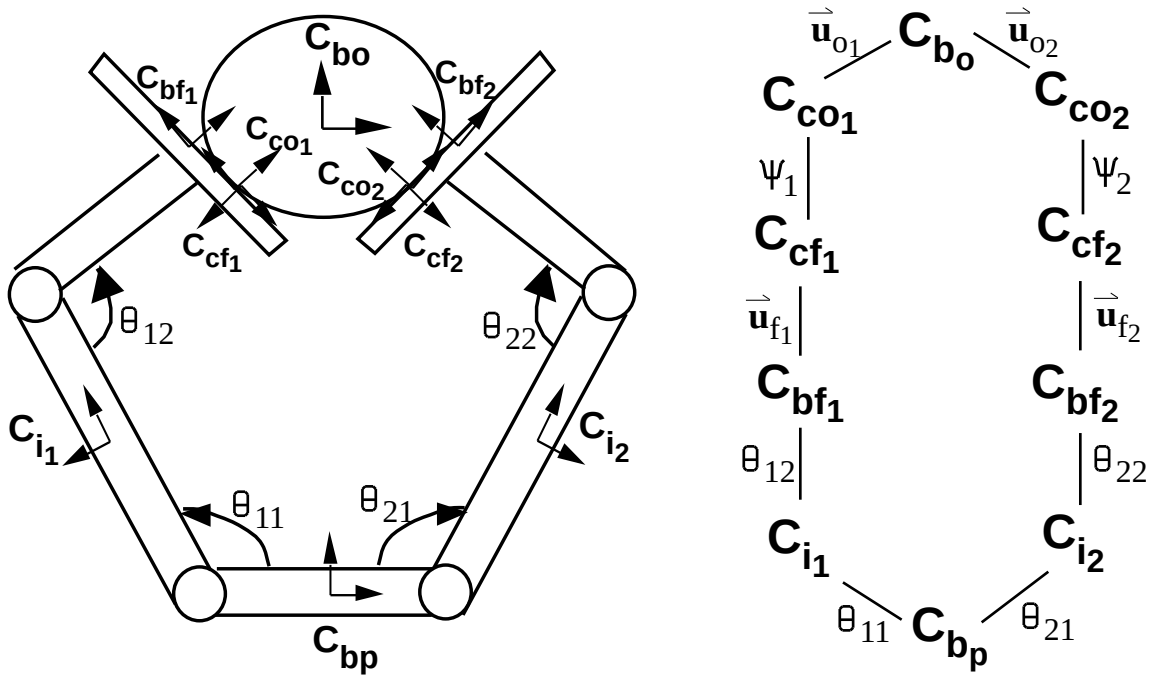

Figure 7: The coordinate frames and full Euclidean graph for a "planar manipulator" grasping a spherical object.

When working with velocities, it is usually more convenient to change basis and use the contact velocity $\tilde{\vec{v}}_{ci}$ rather than $\dot{\vec{\phi}}_i$ because the physical constraints (see Section 3.3.2) are usually most naturally expressed using this basis. With respect to this basis, the velocity is

$$\vec{v}_{e_i} = \gamma_2(T_{c_i}) J_{f_i} \dot{\vec{\theta}}_i + \gamma_2(T_{c_{io}}^{-1}) \tilde{\vec{v}}_{ci} \tag{33}$$

where $T_{c_{io}}$ is the transformation from the frame C_{bo} to the frame C_{co_i}. The Jacobian relative to this basis is

$$\tilde{J}_{e_i} = [\gamma_2(T_{c_i}) J_{f_i}, \gamma_2(T_{c_{io}}^{-1})] \tag{34}$$

The problem with the contact velocity is that it in not the derivative of any state vector. Hence, to determine the system's evolution in configuration space, we must transform from $\tilde{\vec{v}}_{ci}$ to $\dot{\vec{\theta}}_i$.

The constraints due to the closure of the graph of the full system are succinctly expressed in terms of the extended fingers in the following theorem

Theorem 3 *(Fundamental Theorem)*

$$T_{e_1} = T_{e_2} = \cdots = T_{e_m} \tag{35}$$

The instantaneous version of these constraints can be written
Corrolary to Theorem 3

$$J_{e_1} \begin{bmatrix} \dot{\vec{\theta}}_1 \\ \dot{\vec{\phi}}_1 \end{bmatrix} = J_{e_2} \begin{bmatrix} \dot{\vec{\theta}}_2 \\ \dot{\vec{\phi}}_2 \end{bmatrix} = \cdots = J_{e_m} \begin{bmatrix} \dot{\vec{\theta}}_m \\ \dot{\vec{\phi}}_m \end{bmatrix} \tag{36}$$

or relative to the contact velocity basis

$$\tilde{J}_{e_1} \begin{bmatrix} \dot{\vec{\theta}}_1 \\ \tilde{\vec{v}}_{c1} \end{bmatrix} = \tilde{J}_{e_2} \begin{bmatrix} \dot{\vec{\theta}}_2 \\ \tilde{\vec{v}}_{c2} \end{bmatrix} = \cdots = \tilde{J}_{e_m} \begin{bmatrix} \dot{\vec{\theta}}_m \\ \tilde{\vec{v}}_{cm} \end{bmatrix} \tag{37}$$

3.2 Configuration Space

The configuration space of the fingers-plus-object system is the set of all legal combinations of finger joint angles and contact states. Theorem 3 places constraints on which combinations of joint angles and contact states are considered legal; any combination which does not satisfy the closure constraint of Equation 35 is not legal. There are a variety of potential additional constraints on which combinations of joint angles and contact states are legal which arise due to physical constraints on the system. We call these additional constraints "generalized joint limits" (following [16]) because they are analogous to the joint limits of an open-chain manipulator.

There are at least four sources of generalized joint limits: (i) the joint limits on the individual joints of the fingers, (ii) the limits on the locations of the contact points on the fingers, (iii) the limits on the locations of the contact points on the object, and (iv) the solidity of fingers and objects. We now discuss each of these.

Joint limits are constraints on the state of individual physical joints. For example, a revolute joint might be constrained to have angle between 90^o and 270^o, or a linear joint might be constrained to have position between 0 inches and 24 inches. A joint limit affects the configuration space by placing a range on the possible values of a particular entry of some $\vec{\theta}_i$.

In addition to limits on the physical joints, there are also limits on the "virtual joints" associated with contact. One set of virtual joint limits is the limits on the positions of the contact points on the fingertips. The primary constraint on the contact points is that they remain on the fingertips, i.e. on the outermost links of the fingers. Otherwise, degrees of freedom are lost. There can also be spots on the fingertips which are undersirable locations for contact points. For example, on human fingertips, fingernails are a particularly bad place for a contact point to be because of their hardness, slipperiness, and lack of high-resolution tactile sensing.

Another set of virtual joint limits is the limits on the positions of the contact points on the object. In order to use the control schemes of Sections 3.3 and 3.4, the object needs to be fully constrained by the contact. Whether the object is fully constrained depends on the positions of the contact points on the object as well as the type of contact and characteristics of the contact (e.g., coefficient of friction). When there are frictional contacts, the condition that the object be fully constrained by the contact is called "frictional form closure" [4].

The solidity of the fingers and object imposes yet another constraint on possible configurations. Any configuration of the fingers-plus-object system which would have two fingers or a finger and an object occupying the same space is forbidden.

3.3 Kinematics-Based Velocity Control

In this section we discuss one way to move through configuration space: kinematics-based velocity control. By velocity control, we mean that all fingertips remain in contact with the object and that the system state changes continuously as a function of time. By kinematics-based, we mean that there are sufficient constraints on the contact states that the unactuated contact degrees of freedom (and hence the velocity of the object through space) are fully determined by the finger joint velocities; therefore, we can control the full system by controlling the finger joints.

We discuss the two types of constraints on the contact velocities, closure constraints and physical constraints, in Sections 3.3.1 and 3.3.2 respectively. The closure constraints are those which arise from the constraint that the full system be a closed kinematic chain (as discussed in Section 3.1), while the physical constraints result from the physics of contact. Note that for each point of contact there must be a total of six independent constraints: five to fully determine the evolution of the contact state and one to ensure that contact is maintained. (As we discuss in Section 3.4, it is certainly possible for contact points to be lost.)

Section 3.3.3 discusses two different goals for velocity-based manipulation and how to achieve them. The first goal is to control the velocity of the object through space (or, more precisely, relative to the reference frame of the hand). The second goal is to control the motion of the contact points across the object's surface. Unless the fingers have a full six degrees of freedom, these goals are mutually exclusive.

3.3.1 Closure Constraints

The closure constraints are given by Equation 37. After some algebraic manipulation, we can rewrite these constraints as a single equation which explicitly shows the dependence of the contact degrees of freedom on the finger joints

$$\tilde{J}_c \tilde{\vec{v}}_c = J_f \dot{\vec{\theta}} \tag{38}$$

where

$$\tilde{\vec{v}}_c = \begin{bmatrix} \tilde{\vec{v}}_{c1} \\ \cdots \\ \tilde{\vec{v}}_{cm} \end{bmatrix}, \quad \tilde{J}_c = \begin{bmatrix} \gamma_2(T_{c_{1o}}^{-1} T_{c_2}^{-1}) & -\gamma_2(T_{c_{2o}} T_{c_2}^{-1}) & 0 & \cdots & 0 \\ \gamma_2(T_{c_{1o}}^{-1} T_{c_3}^{-1}) & 0 & -\gamma_2(T_{c_{3o}} T_{c_3}^{-1}) & & 0 \\ \cdots & \cdots & 0 & \cdots & 0 \\ \gamma_2(T_{c_{1o}}^{-1} T_{c_m}^{-1}) & 0 & 0 & \cdots & -\gamma_2(T_{c_{mo}} T_{c_m}^{-1}) \end{bmatrix} \tag{39}$$

$$\dot{\vec{\theta}} = \begin{bmatrix} \dot{\vec{\theta}}_1 \\ \cdots \\ \dot{\vec{\theta}}_m \end{bmatrix}, \quad J_f = \begin{bmatrix} -\gamma_2(T_{f_1}^{-1} T_{f_2}) J_{f_1} & J_{f_2} & 0 & \cdots & 0 \\ -\gamma_2(T_{f_1}^{-1} T_{f_3}) J_{f_1} & 0 & J_{f_3} & & 0 \\ \cdots & \cdots & 0 & \cdots & 0 \\ -\gamma_2(T_{f_1}^{-1} T_{f_m}) J_{f_1} & 0 & 0 & \cdots & J_{f_m} \end{bmatrix} \tag{40}$$

Note that the $(i-1)^{st}$ row of Equation 38 expresses the constraint that the velocities of the chains $C_{bf_1} \to C_{bp} \to C_{bf_i}$ and $C_{bf_1} \to C_{bo} \to C_{bf_i}$ are equal.

As long as $\tilde{J}_c$ has full rank, we can think of Equation 38 as $6(m-1)$ constraints on the contact velocities $\tilde{\vec{v}}_c$ selectable by our choice of the joint velocities $\dot{\vec{\theta}}$. In the special case when $\text{rank}(\tilde{J}_c) < 6(m-1)$, Equation 38 provides $\text{rank}(\tilde{J}_c)$ constraints on $\tilde{\vec{v}}_c$ and $6(m-1) - \text{rank}(\tilde{J}_c)$ constraints on $\dot{\vec{\theta}}$.

Example 3 For the configuration of the planar manipulator shown in Figure 8,

$$J_f = \begin{bmatrix} -4 & -7 & 0 & 3 \\ 0 & 0 & 0 & 0 \\ -3\sqrt{3} & 0 & -3\sqrt{3} & 0 \\ 0 & 0 & 0 & 0 \\ 1 & 1 & 1 & 1 \\ 0 & 0 & 0 & 0 \end{bmatrix}, \quad \dot{\vec{\theta}} = \begin{bmatrix} \dot{\theta}_{11} \\ \dot{\theta}_{12} \\ \dot{\theta}_{21} \\ \dot{\theta}_{22} \end{bmatrix} \tag{41}$$

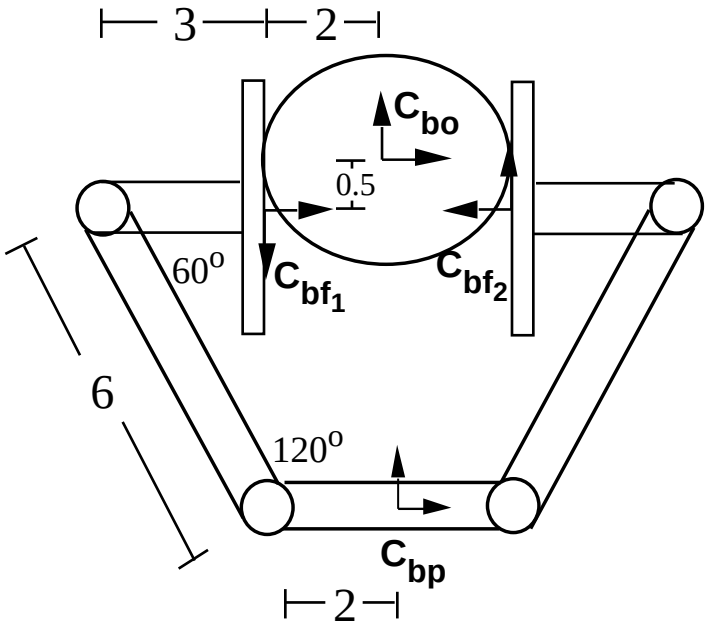

Figure 8: A grasp configuration of the planar manipulator.

$$\tilde{J}_c = \begin{bmatrix} 1 & 0 & 0 & 0 & -4 & 0 & 1 & 0 & 0 & 0 & 0 & 0 \\ 0 & 1 & 0 & 4 & 0 & -0.5 & 0 & -1 & 0 & 0 & 0 & -0.5 \\ 0 & 0 & 1 & 0 & 0.5 & 0 & 0 & 0 & 1 & 0 & -0.5 & 0 \\ 0 & 0 & 0 & 1 & 0 & 0 & 0 & 0 & 0 & 1 & 0 & 0 \\ 0 & 0 & 0 & 0 & 1 & 0 & 0 & 0 & 0 & 0 & -1 & 0 \\ 0 & 0 & 0 & 0 & 0 & 1 & 0 & 0 & 0 & 0 & 0 & 1 \end{bmatrix} \tag{42}$$

3.3.2 Physical Constraints

The closure constraints provide at most $6(m-1)$ constraints on the $6m$ degrees of freedom of the contact velocities. Hence, the contact velocities always require additional constraints to be fully determined. These additional constraints are the "physical constraints", which arise from the physics of the system. Often, these constraints can be expressed in purely kinematic terms (i.e., without reference to the system dynamics), and if there are sufficient kinematic physical constraints (in general, six or more), then the contact velocities are kinematically determined.

Some examples of purely kinematic physical constraints are the following. Point contact with friction produces two kinematic physical constraints, $\tilde{v}_{c_{ix}} = 0$ and $\tilde{v}_{c_{iy}} = 0$, where the contact velocity has components given by $\tilde{\vec{v}}_{c_i} = [\tilde{v}_{c_{ix}}, \tilde{v}_{c_{iy}}, \tilde{v}_{c_{iz}}, \tilde{\omega}_{c_{ix}}, \tilde{\omega}_{c_{iy}}, \tilde{\omega}_{c_{iz}}]^T$. Soft fingertip contact has three kinematic physical constraints, $\tilde{v}_{c_{ix}} = 0$, $\tilde{v}_{c_{iy}} = 0$, and $\tilde{\omega}_{c_{iz}} = 0$. Rigid conforming contact produces five kinematic physical constraints, $\tilde{v}_{c_{ix}} = 0$, $\tilde{v}_{c_{iy}} = 0$, $\tilde{\omega}_{c_{ix}} = 0$, $\tilde{\omega}_{c_{iy}} = 0$ and $\tilde{\omega}_{c_{iz}} = 0$. Adhesive contact has six kinematic constraints, $\tilde{\vec{v}}_{c_i} = 0$.

Rigid conforming contact and adhesive contact require special-purpose grippers. The electrorheological fingertips developed by Kenaley and Cutkosky [10] can create rigid conforming contact. Fingertips with suction cups, glue, or velcro can produce adhesive contact. Standard fingertips usually produce one of: (i) point contact with friction, (ii) soft fingertip contact, or (iii) free contact (i.e., no kinematic physical constraints). Which one is produced depends on the type of translational and rotational friction at the

contact. For kinetic translational and kinetic rotational friction, there is free contact; for static translational and kinetic rotational, there is point contact with friction; for static translational and kinetic rotational, there is soft fingertip contact. With human-like fingertips it is possible to select the contact type for each fingertip by appropriate choice of the internal grasping forces.

Observe that the kinematic physical constraints of all the types of contact discussed above are linear. Hence, for these cases, all the kinematic physical constraints on finger i can be expressed as

$$\tilde{Q}_i \tilde{\vec{v}}_{c_i} = 0 \tag{43}$$

where $\tilde{Q}_i$ is a matrix with as many rows as there are kinematic physical constraints. The full set of physical constraints on the system is given by

$$\tilde{Q}\tilde{\vec{v}}_c = \mathrm{diag}(\tilde{Q}_1, \ldots, \tilde{Q}_m)\tilde{\vec{v}}_c = 0 \tag{44}$$

We can express the closure constraints and kinematic physical constraints jointly as

$$\begin{bmatrix} \tilde{J}_c \\ \tilde{Q} \end{bmatrix} \tilde{\vec{v}}_c = \begin{bmatrix} J_f \\ 0 \end{bmatrix} \dot{\vec{\theta}} \tag{45}$$

If $\mathrm{rank}(\begin{bmatrix} \tilde{J}_c \\ \tilde{Q} \end{bmatrix}) = 6m$, then the contact velocities are kinematically determined; if $\mathrm{rank}(\begin{bmatrix} \tilde{J}_c \\ \tilde{Q} \end{bmatrix}) < 6m$, then the contact velocities are kinematically underdetermined.

Let $\{\tilde{\vec{v}}_{c_{i1}}, \ldots, \tilde{\vec{v}}_{c_{ik}}\}$ be a basis for the space of all possible contact velocities at contact point i which satisfy Equation 43. Then, we call $\tilde{\vec{v}}_{c_{i1}}, \ldots, \tilde{\vec{v}}_{c_{ik}}$ "instantaneous virtual joints" because they span the space of physically possible instantaneous motions which maintain contact. We define the "reduced Jacobian" $\tilde{J}_{r_i}$ such that the velocity $\vec{v}_{c_i}$ of the virtual kinematic chain of contact point i is

$$\vec{v}_{c_i} = \tilde{J}_{r_i} \tilde{\vec{v}}_{cr_i} \tag{46}$$

where $\tilde{\vec{v}}_{cr_i}$ is the representation of the contact velocity relative to the instantaneous virtual joints. When the contact velocities are kinematically determined, we say that the instantaneous virtual joints are "passively actuated" because for any desired finger joint velocities and contact velocities which together satisfy all the constraints, actuating the finger joints to achieve the desired joint velocities forces the contact velocities to be as desired. (This is a generalization of Kerr and Roth's [11] original observation that the contact degrees of freedom are instantaneously equivalent to a spherical joint when there is point contact with friction and Hunt and Torfason's [8] insight about the indirect control of such a "virtual spherical joint.")

When the contact velocities are kinematically underdetermined, we must consider the dynamics of the system to determine which of the kinematically possible values the contact velocities will assume. Hence, the dynamics can be thought of as additional constraints which fully determine a system which is deterministic and kinematically underdetermined. A discussion of dynamics is beyond the scope of this paper, and the interested reader is referred to [17]. The fact that the contact velocities are partially constrained will in some cases allow a simplification of the dynamics.

Example 4 Consider the planar manipulator in Figure 8 with soft fingertip contact at both contact points. Then,

$$\tilde{Q} = \begin{bmatrix} 1 & 0 & 0 & 0 & 0 & 0 & 0 & 0 & 0 & 0 & 0 & 0 \\ 0 & 1 & 0 & 0 & 0 & 0 & 0 & 0 & 0 & 0 & 0 & 0 \\ 0 & 0 & 0 & 0 & 0 & 1 & 0 & 0 & 0 & 0 & 0 & 0 \\ 0 & 0 & 0 & 0 & 0 & 0 & 1 & 0 & 0 & 0 & 0 & 0 \\ 0 & 0 & 0 & 0 & 0 & 0 & 0 & 1 & 0 & 0 & 0 & 0 \\ 0 & 0 & 0 & 0 & 0 & 0 & 0 & 0 & 0 & 0 & 0 & 1 \end{bmatrix} \tag{47}$$

Hence, $\text{rank}(\begin{bmatrix} \tilde{J}_c \\ \tilde{Q} \end{bmatrix}) = 12$, and the contact degrees of freedom are fully constrained. For contact point 1, the virtual instantaneous joints, $\tilde{\vec{v}}_{c_{11}}$ and $\tilde{\vec{v}}_{c_{12}}$, the representation relative to the virtual instantaneous joints, $\tilde{\vec{v}}_{cr_1}$, and the reduced Jacobian, $\tilde{J}_{r_1}$ are

$$\tilde{\vec{v}}_{c_{11}} = \begin{bmatrix} 0 \\ 0 \\ 0 \\ 1 \\ 0 \\ 0 \end{bmatrix}, \quad \tilde{\vec{v}}_{c_{12}} = \begin{bmatrix} 0 \\ 0 \\ 0 \\ 0 \\ 1 \\ 0 \end{bmatrix}, \quad \tilde{\vec{v}}_{cr_1} = \begin{bmatrix} \tilde{\omega}_{c_{1x}} \\ \tilde{\omega}_{c_{1y}} \end{bmatrix}, \quad \tilde{J}_{r_1} = \begin{bmatrix} 0 & 0.5 \\ -2 & 0 \\ 0 & -2 \\ 0 & 0 \\ 0 & 1 \\ -1 & 0 \end{bmatrix} \tag{48}$$

3.3.3 Manipulation Paradigms

In the previous two sections, we discussed how to control the contact velocities. In this section, we examine a few types of manipulation we can perform based on this capability.

One type of manipulation is to control the velocity of the object relative to the palm with kinematically determined contact velocities. (This is the type of manipulation discussed in [18], [11] and [8].) To obtain a desired velocity $\vec{v}$ for the object, we need the velocity for each extended finger to be $\vec{v}$, i.e.

$$\vec{v} = J_{e_i} \begin{bmatrix} \dot{\vec{\theta}}_i \\ \dot{\vec{\phi}}_i \end{bmatrix} \tag{49}$$

for all i. With the closure constraints as expressed in Equation 37, it is clear that the velocities will satisfy these constraints. To find the desired values for the joint and virtual joint velocities, we first express Equation 49 in its reduced form to ensure compliance with the physical constraints

$$\vec{v} = \begin{bmatrix} \gamma_2(T_{c_i}) J_{f_i} & \tilde{J}_{r_i} \end{bmatrix} \begin{bmatrix} \dot{\vec{\theta}}_i \\ \tilde{\vec{v}}_{cr_i} \end{bmatrix} = \tilde{J}_{er_i} \begin{bmatrix} \dot{\vec{\theta}}_i \\ \tilde{\vec{v}}_{cr_i} \end{bmatrix} \tag{50}$$

When $\text{rank}(\tilde{J}_{er_i}) = 6$ for all i, we can for any $\vec{v}$ find values of $\dot{\vec{\theta}}_i$ and $\tilde{\vec{v}}_{cr_i}$ for all i which satisfy Equation 50; therefore, we can move the object with arbitrary velocity relative to the palm. (Note that human fingers all have four degrees of freedom and hence will generally have $\text{rank}(\tilde{J}_{er_i}) = 6$ for any of the three standard contact types.) When $\text{rank}(\tilde{J}_{er_i}) < 6$ for any i, the set of possible velocities of the object is restricted to have dimension < 6. When $\dim(\begin{bmatrix} \dot{\vec{\theta}}_i \\ \tilde{\vec{v}}_{r_i} \end{bmatrix}) > \text{rank}(\tilde{J}_{er_i})$, there are not unique values for $\dot{\vec{\theta}}_i$ and $\tilde{\vec{v}}_{cr_i}$ but rather an infinite set of possible values.

A second type of manipulation is to control the contact velocities and hence the velocities of the points of contact across the surfaces of the object and fingertips [15]. An example of this type of manipulation is grasp adjustment. To achieve particular contact velocities $\tilde{\vec{v}}_c$ which satisfy the physical constraints, we use Equation 38 to solve for the desired joint velocities $\tilde{\vec{v}}_f$. If the contact velocities are kinematically determined, they automatically assume the values $\tilde{\vec{v}}_c$. (This is a generalization of Montana's result for two fingers [15].) If the contact velocities are kinematically underdetermined, one must additionally control the dynamics. (Cole, Hsu and Sastry [5] discuss one method for this.) If $\text{rank}(J_f) = 6(m-1)$, then any contact velocities are achievable. If $\text{rank}(J_f) < 6(m-1)$, then a restricted set of contact velocities is achievable. If $\dim(\vec{v}_f) > \text{rank}(J_f)$, then there are redundant degrees of freedom which can be chosen as desired.

3.4 Hyperspace Jumps

While pure kinematics-based velocity control is often sufficient for moving the object small distances (or angles), large motions often require additional control strategies. This is because, in general, moving the object with a constant velocity will eventually cause a generalized joint limit to be reached. In this section, we describe a different control strategy, the hyperspace jump, which when used in conjunction with kinematics-based velocity control allows execution of large motions while avoiding generalized joint limits.

A hyperspace jump is when one or more of the fingertips break contact and re-engage in a different state. (We call such a maneuver a "hyperspace jump" because it is a jump from one point in space to another obtained by going through a higher-dimensional embedding space.) While these fingertips lose contact, the other fingertips maintain their grasp on the object. Although the fingers that remain in contact may continue to move the object, the true objective of a hyperspace jump is to change the extended state, i.e. joint angles and contact states, of the fingers which break contact. With proper planning, a combination of kinematics-based velocity control and hyperspace jumps will produce the desired motion of the object while avoiding generalized joint limits. Section 3.5 shows an example of how this works.

Hyperspace jumps are actually very similar to the particular type of kinematics-based velocity control which occurs when a subset of the fingers are grasping the object and the others are moving with free contact, i.e. with no physical constraints. However, there are two differences between free contact and no contact. First and foremost, fingers moving with free contact are still confined to meet the generalized joint limits, while fingers moving with no contact can pass over generalized joint limits to topologically disconnected portions of configuration space. Second, moving with free contact still induces dynamic interactions between the fingertip and object, while moving with no contact does not.

3.5 An Example: Twirling a Baton

We now present an example of how kinematics-based velocity control and hyperspace jumps can be used to plan a trajectory through the configuration space. The task is twirling a baton, a task which was originally discussed and implemented by Fearing [6]. The object in this task is a cylinder with radius r_o and height h. The goal of the task is to manipulate the object so that it rotates around an axis through its center and perpendicular to its length for an arbitrarily large number of rotations in a single direction.

The hand uses three fingers. We choose the geometry and kinematics of the fingers to make the mathematics involved as simple as possible and hence not to lose the central ideas in the mathematical details. The fingertips of these fingers are identically shaped and, over their legal areas of contact, are shaped like cylinders with radius r_f, where $r_f < h/\pi$. (As we will see, the contact points move on the object, and this bound on the size of the fingertips is required to provide sufficient room to move.) The fingers are three-degree-of-freedom Cartesian manipulators and hence can move the fingertip with any translational velocity (respecting generalized joint limits and joint velocity limits) but with no rotational velocity. The contact is soft contact with friction when there are two fingers contacting the object (thus allowing the fingers to constrain the object during a hyperspace jump) and point contact with friction when there are three fingers contacting the object (thus giving the extended fingers six degrees of freedom during velocity control phases). (A possible physical explanation of this in contact type is that the force exerted by the fingers is greater when there are two fingers contacting than when there are three fingers contacting.)

To perform the task, the hand is positioned so that the axes of the fingertips are oriented parallel to the axis of rotation. As we will see, for the entire task the contact points remain in the plane perpendicular to this axis through the center of the object. Therefore, we can illustrate the motion of the fingertips,

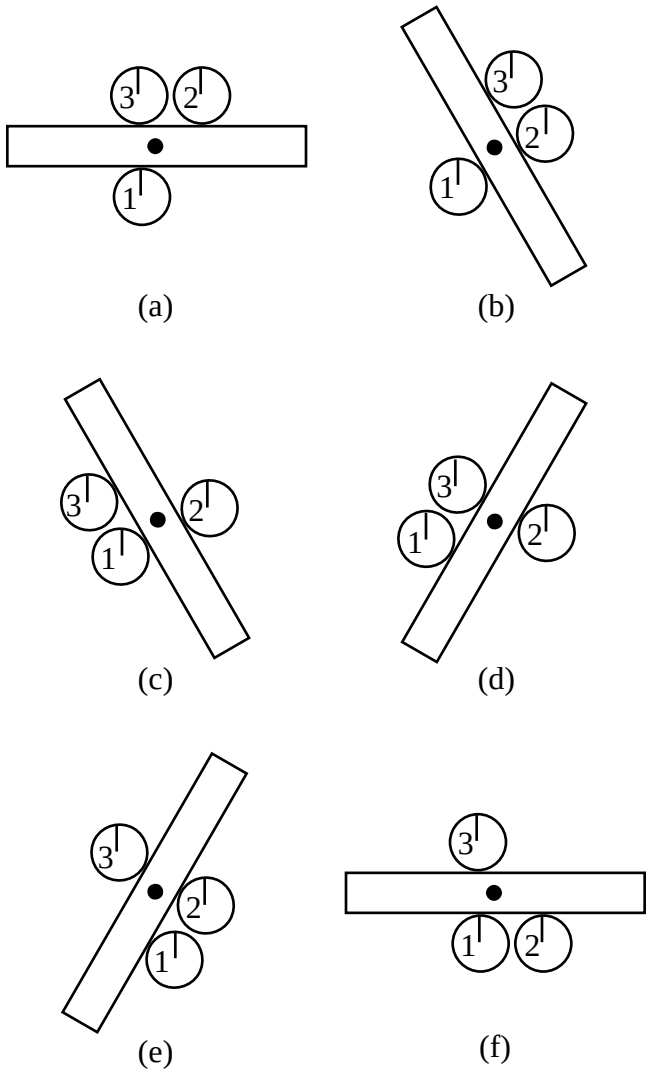

Figure 9: Alternating between kinematics-based velocity control and hyperspace jumps, the system cycles through this sequence of configurations.

object, and contact points with two-dimensional slices through this plane. This is exactly what we do in Figure 9, which illustrates the sequence of system configurations as the fingers use a combination of velocity control and hyperspace jumps to rotate the object half a turn and end up back in the same basic configuration as where they started. We now discuss the motions depicted in Figure 9 in detail, paying special attention to the transition from configuration a to configuration b and the transition from configuration b to configuration c because the other transitions are similar to these.

Transition from configuration a to configuration b: Configuration a shows the initial grasp configuration. From this initial configuration, we perform kinematics-based velocity control to rotate the object through an angle of $-\pi/3$ around its center, after which the system ends up in configuration b. The key question then is how to choose the joint velocities so as to achieve the desired object motion. In Section 3.3.3, we saw that Equation 50 allowed us to calculate these joint velocities. However, the problem is that the Jacobian terms in this equation change as a function of time. Because $\tilde{J}_{r_i}$ and $\gamma_2(T_{c_i})$ are functions of the position of the contact points, we need to compute these positions (or, in an actual hand with tactile-sensing fingertips, sense these positions) as a function of time. Because of the way we have chosen the geometry and kinematics for this example, the velocities of the contact points are constant throughout the trajectory. Hence, we can compute them first and then use them to compute the joint velocities as a function of time.

Computation of the induced contact point velocities: In order to apply Equation 27 of Theorem 2, we first need to choose coordinate patches for the surfaces of the object and the fingertips. Since they are all cylinders, we can use for all of them the following coordinate system for a cylinder of radius r and height h:

$$U = \{(u,v) | -h/2 < u < h/2, -\pi r < v < \pi r\}, \quad f(u,v) = (r\cos(v/r), r\sin(v/r), u) \tag{51}$$

Then, the curvature, torsion and scale matrix are:

$$K = \mathrm{diag}(0, 1/r), \quad Q = 0, \quad M = I \tag{52}$$

Assume that in configuration a the contact points are placed so that for contact point i the positions $\vec{u}_{f_i}$ and $\vec{u}_{o_i}$ on the finger and object respectively are:

$$\vec{u}_{f_1} = (0, -\pi r_f/6), \quad \vec{u}_{o_1} = (-\pi r_f/6, r_o\pi) \tag{53}$$

$$\vec{u}_{f_2} = (0, -\pi r_f/2), \quad \vec{u}_{o_2} = (\pi r_f/2, 0) \tag{54}$$

$$\vec{u}_{f_3} = (0, \pi r_f/6), \quad \vec{u}_{o_3} = (-\pi r_f/6, 0) \tag{55}$$

Further assume that the directions of increasing x component of $\vec{u}$ are out of the page and to the right for the fingers and the object respectively. (The direction of increasing y component can be inferred by knowing that the z direction is outwardly normal and the induced Gauss coordinate frame must be right-handed.) Then, the values of the angle ψ_i at the three contact points are

$$\psi_1 = -\pi/2, \quad \psi_2 = \psi_3 = \pi/2 \tag{56}$$

and the contact velocities $\tilde{\vec{v}}_i$ at the three points are

$$\tilde{\vec{v}}_1 = (0,0,0,0,-\omega_0,0)^T, \quad \tilde{\vec{v}}_2 = \tilde{\vec{v}}_3 = (0,0,0,0,\omega_0,0)^T \tag{57}$$

where ω_0 is the magnitude of the angular velocity of the object. According to Equation 28,

$$\tilde{J}_1 = \begin{bmatrix} -1 & 0 & 0 & 1 & 0 \\ 0 & -1 & 1 & 0 & 0 \\ 0 & 0 & 0 & 0 & 0 \\ 0 & 1/r_o & 0 & 0 & 0 \\ 0 & 0 & 0 & -1/r_f & 0 \\ 0 & 0 & 0 & 0 & 1 \end{bmatrix}, \quad \tilde{J}_2 = \tilde{J}_3 = \begin{bmatrix} -1 & 0 & 0 & -1 & 0 \\ 0 & -1 & -1 & 0 & 0 \\ 0 & 0 & 0 & 0 & 0 \\ 0 & 1/r_o & 0 & 0 & 0 \\ 0 & 0 & 0 & 1/r_f & 0 \\ 0 & 0 & 0 & 0 & 1 \end{bmatrix} \tag{58}$$

Applying Equation 27 and solving for the $\dot{\vec{\phi}}_i$ gives

$$\dot{\vec{\phi}}_1 = \begin{bmatrix} \dot{\vec{u}}_{o_1} \\ \dot{\vec{u}}_{f_1} \\ \dot{\psi}_1 \end{bmatrix} = \begin{bmatrix} r_f\omega_o \\ 0 \\ 0 \\ r_f\omega_o \\ 0 \end{bmatrix}, \quad \dot{\vec{\phi}}_2 = \begin{bmatrix} \dot{\vec{u}}_{o_2} \\ \dot{\vec{u}}_{f_2} \\ \dot{\psi}_2 \end{bmatrix} = \dot{\vec{\phi}}_3 = \begin{bmatrix} \dot{\vec{u}}_{o_3} \\ \dot{\vec{u}}_{f_3} \\ \dot{\psi}_3 \end{bmatrix} = \begin{bmatrix} -r_f\omega_o \\ 0 \\ 0 \\ r_f\omega_o \\ 0 \end{bmatrix} \tag{59}$$

Assuming that ω_0, the angular velocity of the object, is constant, then for $0 \leq t \leq \pi/(3\omega_0)$ the contact points are at

$$\vec{u}_{f_1} = (0, -\pi r_f/6 + t r_f \omega_0), \quad \vec{u}_{o_1} = (-\pi r_f/6 + t r_f \omega_0, r_o \pi) \tag{60}$$

$$\vec{u}_{f_2} = (0, -\pi r_f/2 + t r_f \omega_0), \quad \vec{u}_{o_2} = (\pi r_f/2 - t r_f \omega_0, 0) \tag{61}$$

$$\vec{u}_{f_3} = (0, \pi r_f/6 + t r_f \omega_0), \quad \vec{u}_{o_3} = (-\pi r_f/6 - t r_f \omega_0, 0) \tag{62}$$

Computation of the joint velocities: Assume that C_{bp}, the base coordinate frame of the hand, is oriented so that $\vec{x}$ is right, $\vec{y}$ is out of the paper, and $\vec{z}$ is down. Also assume that the joint 1 of each finger is a linear joint oriented in the x direction relative to this base coordinate frame, joint 2 is a linear joint oriented in the y direction, and joint 3 is a linear joint oriented in the z direction. Then, knowing the positions of the contact points, we can compute the terms $\tilde{J}_{er_i}$ in Equation 50

$$\tilde{J}_{er_1} = \begin{bmatrix} \cos(\omega_0 t) & 0 & \sin(\omega_0 t) & 0 & -r_o & 0 \\ 0 & 1 & 0 & r_o & 0 & \pi r_f/6 - t r_f \omega_0 \\ -\sin(\omega_0 t) & 0 & \cos(\omega_0 t) & 0 & t r_f \omega_0 - \pi r_f/6 & 0 \\ 0 & 0 & 0 & 1 & 0 & 0 \\ 0 & 0 & 0 & 0 & 1 & 0 \\ 0 & 0 & 0 & 0 & 0 & 1 \end{bmatrix} \tag{63}$$

$$\tilde{J}_{er_2} = \begin{bmatrix} \cos(\omega_0 t) & 0 & \sin(\omega_0 t) & 0 & -r_o & 0 \\ 0 & -1 & 0 & r_o & 0 & t r_f \omega_0 - \pi r_f/2 \\ \sin(\omega_0 t) & 0 & -\cos(\omega_0 t) & 0 & \pi r_f/2 - t r_f \omega_0 & 0 \\ 0 & 0 & 0 & 1 & 0 & 0 \\ 0 & 0 & 0 & 0 & 1 & 0 \\ 0 & 0 & 0 & 0 & 0 & 1 \end{bmatrix} \tag{64}$$

$$\tilde{J}_{er_3} = \begin{bmatrix} \cos(\omega_0 t) & 0 & \sin(\omega_0 t) & 0 & -r_o & 0 \\ 0 & -1 & 0 & r_o & 0 & t r_f \omega_0 + \pi r_f/6 \\ \sin(\omega_0 t) & 0 & -\cos(\omega_0 t) & 0 & -\pi r_f/6 - t r_f \omega_0 & 0 \\ 0 & 0 & 0 & 1 & 0 & 0 \\ 0 & 0 & 0 & 0 & 1 & 0 \\ 0 & 0 & 0 & 0 & 0 & 1 \end{bmatrix} \tag{65}$$

Using the contact velocites from Equation 57, we can substitute into Equation 50 and solve for the joint velocities to get

$$\dot{\vec{\theta}}_1 = \begin{bmatrix} \dot{\theta}_{1x} \\ \dot{\theta}_{1y} \\ \dot{\theta}_{1z} \end{bmatrix} = \begin{bmatrix} -r_o\omega_0\cos(\omega_0 t) + \omega_0(\pi r_f/6 - t r_f\omega_0)\sin(\omega_0 t) \\ 0 \\ -r_o\omega_0\sin(\omega_0 t) - \omega_0(\pi r_f/6 - t r_f\omega_0)\cos(\omega_0 t) \end{bmatrix} \tag{66}$$

$$\dot{\vec{\theta}}_2 = \begin{bmatrix} \dot{\theta}_{2x} \\ \dot{\theta}_{2y} \\ \dot{\theta}_{2z} \end{bmatrix} = \begin{bmatrix} r_o\omega_0\cos(\omega_0 t) + \omega_0(-\pi r_f/2 + t r_f\omega_0)\sin(\omega_0 t) \\ 0 \\ r_o\omega_0\sin(\omega_0 t) - \omega_0(-\pi r_f/2 + t r_f\omega_0)\cos(\omega_0 t) \end{bmatrix} \tag{67}$$

$$\dot{\vec{\theta}}_3 = \begin{bmatrix} \dot{\theta}_{3x} \\ \dot{\theta}_{3y} \\ \dot{\theta}_{3z} \end{bmatrix} = \begin{bmatrix} r_o\omega_0\cos(\omega_0 t) + \omega_0(\pi r_f/6 + t r_f\omega_0)\sin(\omega_0 t) \\ 0 \\ r_o\omega_0\sin(\omega_0 t) - \omega_0(\pi r_f/6 + t r_f\omega_0)\cos(\omega_0 t) \end{bmatrix} \tag{68}$$

Transition from configuration b to configuration c: When the system reaches configuration b, the contact points are at

$$\vec{u}_{f_1} = (0, \pi r_f/6), \quad \vec{u}_{o_1} = (\pi r_f/6, r_o\pi) \tag{69}$$

$$\vec{u}_{f_2} = (0, -\pi r_f/6), \quad \vec{u}_{o_2} = (\pi r_f/6, 0) \tag{70}$$

$$\vec{u}_{f_3} = (0, \pi r_f/2), \quad \vec{u}_{o_3} = (-\pi r_f/2, 0) \tag{71}$$

Continuing with kinematics-based velocity control will soon bring the contact points to a position where there is no longer frictional form closure, i.e. where the generalized joint limits are violated. Therefore, instead of continuing with velocity control, we stop and perform a hyperspace jump. Fingers 1 and 2 remain in contact with the object while finger 3 breaks contact and re-engages in a different configuration. The new contact positions for contact point 3 are

$$\vec{u}_{f_3} = (0, -\pi r_f/2), \quad \vec{u}_{o_3} = (-\pi r_f/2, r_o\pi) \tag{72}$$

There are a variety of paths that finger 3 can travel in order to break contact, travel to the other side of the object, and regain contact. However, whatever the path, the total translation of the fingertip relative to C_{bp}, the base coordinate frame of the hand, is $[-\sqrt{3}(r_o + r_f), 0, r_o + r_f]^T$.

Transition from configuration c to configuration d: This motion uses kinematics-based velocity control. It is similar enough to the transition from a to b that we do not go through all the calculations again but rather just give the resulting finger joint velocities for $0 \le t \le \pi/(3\omega_0)$

$$\begin{bmatrix} \dot{\theta}_{1x} \\ \dot{\theta}_{1y} \\ \dot{\theta}_{1z} \end{bmatrix} = \begin{bmatrix} -r_o\omega_0\cos(\omega_0(t+\pi/3)) + \omega_0(-\pi r_f/6 - t r_f\omega_0)\sin(\omega_0(t+\pi/3)) \\ 0 \\ -r_o\omega_0\sin(\omega_0(t+\pi/3)) - \omega_0(-\pi r_f/6 - t r_f\omega_0)\cos(\omega_0(t+\pi/3)) \end{bmatrix} \tag{73}$$

$$\begin{bmatrix} \dot{\theta}_{2x} \\ \dot{\theta}_{2y} \\ \dot{\theta}_{2z} \end{bmatrix} = \begin{bmatrix} r_o\omega_0\cos(\omega_0(t+\pi/3)) + \omega_0(-\pi r_f/6 + t r_f\omega_0)\sin(\omega_0(t+\pi/3)) \\ 0 \\ r_o\omega_0\sin(\omega_0(t+\pi/3)) - \omega_0(-\pi r_f/6 + t r_f\omega_0)\cos(\omega_0(t+\pi/3)) \end{bmatrix} \tag{74}$$

$$\begin{bmatrix} \dot{\theta}_{3x} \\ \dot{\theta}_{3y} \\ \dot{\theta}_{3z} \end{bmatrix} = \begin{bmatrix} -r_o\omega_0\cos(\omega_0(t+\pi/3)) + \omega_0(\pi r_f/2 - t r_f\omega_0)\sin(\omega_0(t+\pi/3)) \\ 0 \\ -r_o\omega_0\sin(\omega_0(t+\pi/3)) - \omega_0(\pi r_f/2 - t r_f\omega_0)\cos(\omega_0(t+\pi/3)) \end{bmatrix} \tag{75}$$

Transition from configuration d to configuration e: This hyperspace jump which takes fingertip 1 from one side of the object to the other is completely analogous to the transition from b to c. The contact positions start at

$$\vec{u}_{f_1} = (0, \pi r_f/2), \quad \vec{u}_{o_1} = (\pi r_f/2, r_o\pi) \tag{76}$$

$$\vec{u}_{f_2} = (0, \pi r_f/6), \quad \vec{u}_{o_2} = (-\pi r_f/6, 0) \tag{77}$$

$$\vec{u}_{f_3} = (0, -\pi r_f/6), \quad \vec{u}_{o_3} = (-\pi r_f/6, r_o\pi) \tag{78}$$

The new positions for contact point 1 are

$$\vec{u}_{f_1} = (0, -\pi r_f/2), \quad \vec{u}_{o_1} = (\pi r_f/2, 0) \tag{79}$$

Transition from configuration e to configuration f: The finger joint velocities are

$$\begin{bmatrix} \dot{\theta}_{1x} \\ \dot{\theta}_{1y} \\ \dot{\theta}_{1z} \end{bmatrix} = \begin{bmatrix} r_o\omega_0 \cos(\omega_0(t + 2\pi/3)) + \omega_0(-\pi r_f/2 + t r_f \omega_0) \sin(\omega_0(t + 2\pi/3)) \\ 0 \\ r_o\omega_0 \sin(\omega_0(t + 2\pi/3)) - \omega_0(-\pi r_f/2 + t r_f \omega_0) \cos(\omega_0(t + 2\pi/3)) \end{bmatrix} \tag{80}$$

$$\begin{bmatrix} \dot{\theta}_{2x} \\ \dot{\theta}_{2y} \\ \dot{\theta}_{2z} \end{bmatrix} = \begin{bmatrix} r_o\omega_0 \cos(\omega_0(t + 2\pi/3)) + \omega_0(\pi r_f/6 + t r_f \omega_0) \sin(\omega_0(t + 2\pi/3)) \\ 0 \\ r_o\omega_0 \sin(\omega_0(t + 2\pi/3)) - \omega_0(\pi r_f/6 + t r_f \omega_0) \cos(\omega_0(t + 2\pi/3)) \end{bmatrix} \tag{81}$$

$$\begin{bmatrix} \dot{\theta}_{3x} \\ \dot{\theta}_{3y} \\ \dot{\theta}_{3z} \end{bmatrix} = \begin{bmatrix} -r_o\omega_0 \cos(\omega_0(t + 2\pi/3)) + \omega_0(\pi r_f/6 - t r_f \omega_0) \sin(\omega_0(t + 2\pi/3)) \\ 0 \\ -r_o\omega_0 \sin(\omega_0(t + 2\pi/3)) - \omega_0(\pi r_f/6 - t r_f \omega_0) \cos(\omega_0(t + 2\pi/3)) \end{bmatrix} \tag{82}$$

Transition from configuration f to configuration a: This hyperspace jump takes fingertip 2 from one side of the object to the other, thus completing a half-turn of the object and leaving the fingers in a position to continue repeating this procedure indefinitely. The contact positions start at

$$\vec{u}_{f_1} = (0, -\pi r_f/6), \quad \vec{u}_{o_1} = (\pi r_f/6, 0) \tag{83}$$

$$\vec{u}_{f_2} = (0, \pi r_f/2), \quad \vec{u}_{o_2} = (-\pi r_f/2, 0) \tag{84}$$

$$\vec{u}_{f_3} = (0, \pi r_f/6), \quad \vec{u}_{o_3} = (\pi r_f/6, r_o\pi) \tag{85}$$

The new positions for contact point 2 are

$$\vec{u}_{f_2} = (0, -\pi r_f/2), \quad \vec{u}_{o_2} = (-\pi r_f/2, r_o\pi) \tag{86}$$

Note that the contact positions on the object are not the same as the original ones. This is because the object has only completed half a turn. After a second half-turn these positions are back where they started.

4 Conclusion

We have derived a full configuration-space description of the kinematics of multi-fingered manipulation. We have done this by first formulating the contact kinematics as a virtual kinematic chain. Then, we could view the fingers-plus-object system as a large closed virtual kinematic chain. The configuration space of the system, i.e. the set of legal states of the closed kinematic chain, has boundaries determined by a set of constraints called the "generalized joint limits".

We have described two ways to move through the system's configuration space, both of which rely on kinematics-based control, i.e. control under which the system configuration is fully determined by the finger joint angles. (While dynamics-based control fits into our kinematic model, it is beyond the scope of this paper.) The first is kinematics-based velocity control, where all fingertips maintain contact. The key to this type of control is using the combination of kinematic closure constraints and physical contact constraints to indirectly control the unactuated contact degrees of freedom. The second is hyperspace jumps, where some of the fingertips break contact and regain contact in a different configuration while the other fingertips maintain a grasp on the object. The combination of kinematics-based velocity control and hyperspace jumps allows planning of large motions through configuration space which avoid generalized joint limits, as demonstrated in an example showing how to perform the task of twirling a baton.

References

[1] D.L. Brock, "Enhancing the dexterity of a robot hand using controlled slip", *Proc. IEEE Conf. Robotics and Automation,* pp. 249–251, 1988.

[2] R.W. Brockett, *Some mathematical aspects of robotics Robotics: Proceedings of Symposia in Applied Mathematics, Vol. 41*, R.W. Brockett, Ed. Providence, RI: Amer. Math. Soc., pp. 1–19, 1990.

[3] C. Cai and B. Roth, "On the spatial motion of rigid bodies with point contact," *Proc. IEEE Conf. Robotics and Automation,* pp. 686–695, 1987.

[4] C.Z. Chammas. Analysis and implementation of robust grasping behaviors. Master's thesis, MIT Dept. of Mech. Eng., 1990.

[5] A.A. Cole, P. Hsu and S.S. Sastry, "Dynamic control of sliding by robot hands for regrasping," *IEEE Trans. Robotics and Automation*, vol. 8, no. 1, pp. 42–52, 1992.

[6] R.S. Fearing, "Implementing a force strategy for object re-orientation," *Proc. IEEE Conf. Robotics and Automation,* pp. 96–102, 1986.

[7] J. Hong, G. Lafferriere, B. Mishra. and X. Tan, "Fine manipulation with multifinger hands," *Proc. IEEE Conf. Robotics and Automation,* pp. 1568–1573, 1990.

[8] K.H. Hunt and L.E. Torfason, "A three-fingered pantograph manipulator – a kinematic study," *Trans. ASME J. Mech. Transmissions, Automat. Des.*, vol. 109, no. 2, pp. 171–177, 1987.

[9] K.H. Hunt, A.E. Samuel, and P.R. McAree. "Special configurations of multi-finger multi-freedom grippers - a kinematic study," *Int. J. Robotics Research*, vol. 10, no. 2, pp. 123–134, 1991.

[10] G.L. Kenaley and M.R. Cutkosky, "Electrorheological fluid-based robotic fingers with tactile sensing," *Proc. IEEE Conf. Robotics and Automation,* pp. 132–136, 1989.

[11] J. Kerr and B. Roth, "Analysis of multifingered hands," *Int. J. Robotics Research*, vol. 4, no. 4, pp. 3–17, 1986.

[12] Z. Li and S. Sastry, "A unified approach for the control of multifingered robot hands," *Contemporary Mathematics*, vol. 97, pp. 217–239, 1989.

[13] Z. Li and J. Canny, "Motion of two rigid bodies with rolling constraint," *IEEE Trans. Robotics and Automation*, vol. 6, no. 1, pp. 62–72, 1990.

[14] D.J. Montana, *Tactile sensing and the kinematics of contact*, Ph.D. Thesis, Division of Applied Sciences, Harvard University, 1986.

[15] D.J. Montana, "The kinematics of contact and grasp," *Int. J. Robotics Research*, vol. 7, no. 3, pp. 17–32, 1988.

[16] D.J. Montana, "Contact Stability for Two-Fingered Grasps," *IEEE Trans. Robotics and Automation*, vol. 8, no. 4, pp. 421-430, 1992.

[17] R.M. Murray and S.S. Sastry, "Grasping and manipulation using multifingered robot hands," *Robotics: Proceedings of Symposia in Applied Mathematics, Vol. 41*, R.W. Brockett, Ed. Providence, RI: Amer. Math. Soc., pp. 91–128, 1990.

[18] J.K. Salisbury, *Kinematic and Force Analysis of Articulated Hands*, Ph.D. thesis, Stanford University, Dept. of Mechanical Engineering, 1982.

[19] J.C Trinkle and R.P. Paul, "Planning for dextrous manipulation with sliding contacts," *Int. J. Robotics Research*, vol. 9, no. 3, pp. 24–48, 1990.